SOIL EROSION ASSESSMENT AND SIMULATION BY MEANS OF SGEOS AND ANCILLARY DIGITAL DATA

Carsten Jürgens
Michael Fander
University of Trier
FB VI, Geography/Geosciences
Remote Sensing Department
P.O. Box 3825
D-5500 Trier, FRG
ISPRS-Commission IV

ABSTRACT

This study uses the well-known Universal Soil Loss Equation (USLE) to assess the long-term soil erosion in a small catchment area and to simulate various soil protection alternatives.

This raster-oriented study uses a very accurate multitemporal land-use classification to determine the land-cover (C-Factor). The other input variables have been determined from ancillary data (eg. digital elevation model and soil data).
The compiled data layers of this GIS allow the calculation of the long-term soil erosion per pixel as well as inquiries about all data layers for every pixel.

In addition to the resulting soil erosion risk map it is possible to simulate soil protection measures with the computer. This ensures that only the most effective ones are introduced to the field.

Keywords: Landsat TM, Multitemporal Land-use Classification, GIS, Simulation, Soil erosion

1. INTRODUCTION

This paper describes the use of remote sensing techniques and GIS applied in the field of soil erosion.

In this field remote sensing techniques have already been applied. For instance single events (rainstorms, wind) that cause soil erosion have been evaluated. By means of aerial photography such single events have also been quantified.

Nowadays satellite remote sensing becomes more and more popular because of the synoptical view of large areas (which implies cheap large area mapping) and the spectral and radiometric properties of modern earth observation satellites. Since spaceborne sensors have a much poorer spatial resolution than aerial photographs they are unable to show details which are relevant to soil erosion.

However, we can use spaceborne satellite systems to evaluate the long-term soil erosion rates, though we can not study the impact of soil erosion for single events.

By application of the Universal Soil Loss Equation (USLE) (WISCHMEIER & SMITH 1978) we are able to determine the long-term soil erosion. The land-cover (C-factor) is determined by a multi-temporal land-use classification of two satellite images from May and July 1990. The other factors have been determined in the field (K-factor) or by assistance of a digital elevation model (L- and S-factor).

Universal Soil Loss Equation (USLE):

$$A = S \cdot L \cdot R \cdot P \cdot C \cdot K \ [t/ha \cdot a] \qquad (1)$$

A = mean soil loss per year [t/ha·a]
S = slope factor
L = slope length factor
R = rainfall factor
P = practice factor
C = land use/land cover factor
K = soil erodibility factor

2. DIGITAL IMAGE PROCESSING STEPS

For this study system-corrected LANDSAT TM-data from May 3rd and July 15th, 1990 have been purchased for the study area (figure 1).

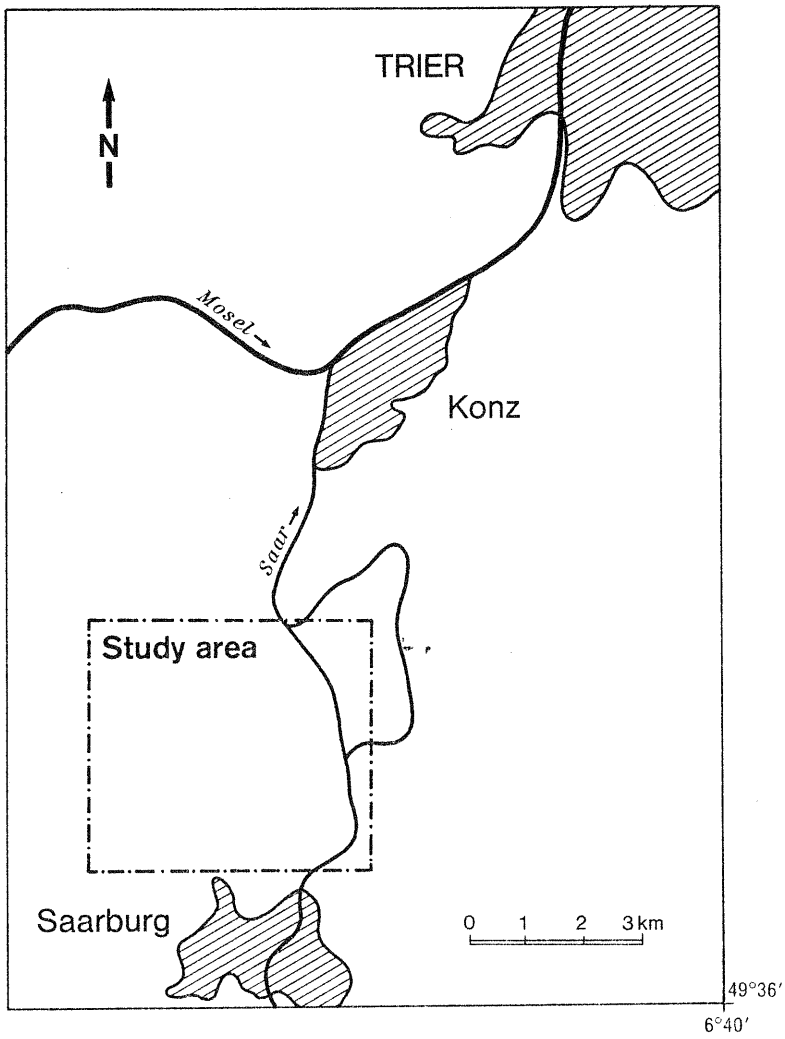

Figure 1: Study area

LANDSAT TM-data have a spatial resolution of 30 m x 30 m in the visible and infrared spectrum except in the thermal infrared.

At first the image data have been geocoded to a map 1:25.000 with Gauß-Krüger-Coordinates (FANDER 1990). The achieved accuracy of the geometric correction and the image registration process is approximately 0.5 pixels. This subpixel accuracy is very precise, as a topographic map overlay proved.

To eleminate redundant information in the twelve spectral bands used (six for each image), a principal component transformation had to be performed.

Prior to that principal component transformation the histograms of the TM-bands had to be standardized (SCHULZ 1988):

$$DN_{neu} = \frac{DN_{alt_i} - \bar{X}_i}{S_{soll_i} + \bar{X}_{soll_{S_i}}} \quad (2)$$

with:

$DN_{neu\ i}$ = standardized Digital Number of TM-band i

$DN_{alt\ i}$ = original Digital Number of TM-band i

$\bar{X}_i$ = arithmetic mean of TM-band i

S_i = standard deviation of TM-band i

$\bar{X}_{soll}$ = arithmetic mean after standardization (here: 90)

S_{soll} = standard deviation after standardization (here: 23)

After standardization the principal component transformation was calculated.

The SCREE-Test revealed that only the first three principal components have to be used for the further studies. These first three principal components represent more than 90 % of the original variance (of 12 TM-bands) inherent in the satellite images.

According to the SCREE-Test it is decided to use only these first three principal components for the classification. This results in a small loss of variance (ca. 9 %) but achieves a data reduction of 75 % which saves a lot of computing time during the classification process since the feature space has been significantly reduced from 12 to three dimensions!

The color-coded principal component image and the topographic map overlay have been used to select training samples in the field, which are needed for the supervised land-use classification.

30 Training Samples have been selected which represent relevant land-use classes in their slightly different spectral appearences. Their spectral signatures have been evaluated very carefully to reach high accuracy in the multitemporal maximum likelihood classification.

For each class a priori probabilities have been determined, so that no overlapping classes occur in the feature space. This is important to reach a high classification accuracy. After the classification had been performed, the accuracy has been checked.

The classification accuracy is between 98 and 100 %. Very few wrong classified pixels occured in the classification result. This high accuracy results in about one third not classified pixels. These from the classifier rejected pixels could not be addressed to one of the established land-use classes due to the high accuracy that was demanded.

It is possible to lower the threshholds for each class to get more classified pixels, but these are mostly wrong classified pixels. So it seems to be better to classify less pixels but guarantie a high accuracy for these pixels.

3. ANCILLARY DIGITAL DATA

Soil data have been acquired in the field. These point data have been used to create a soil map. According to this map an average K-factor per soil has been determined (SCHMIDT 1979). From these soil data also the depth of the soils has been used to create a map. This is important üsince the tolerable soil erosion rate is dependent on the soil depth (after SCHWERTMANN et al. 1987).

A digital elevation model (figure 2) has been used for calculation of S- and L-factors. The following slope classes (table 1) have been used for calculation of S- and L-factors (BARSCH & MÄUSBACHER 1990).

Table 1: Range and mean slope of slope classes

Range	Mean Slope
0 %	0 %
1-4 %	2,5 %
5-12 %	8,5 %
13-27 %	20,0 %
28-70 %	49,0 %
71-103 %	86,5 %

Also the slope length has been determined by assistance of 8 aspect directions (according to 8 aspect classes). For each class the slope length had to be determined.

In the study area no special soil erosion prevention practices are applied. Therefore the P-factor is constantly set to 1.

According to measurements of a meteorological station in Trier and personal communications with R.-G. Schmidt a rainfall-factor of 55 is realistic for the study area.

4. SOIL EROSION CALCULATION

After all these data layers have been established in the GIS (as map and in the data base) they can be multiplied according to the USLE.

5. RESULTS

The following summary table (table 2) shows the correlation of land-use classes and their soil erosion contribution in percent.

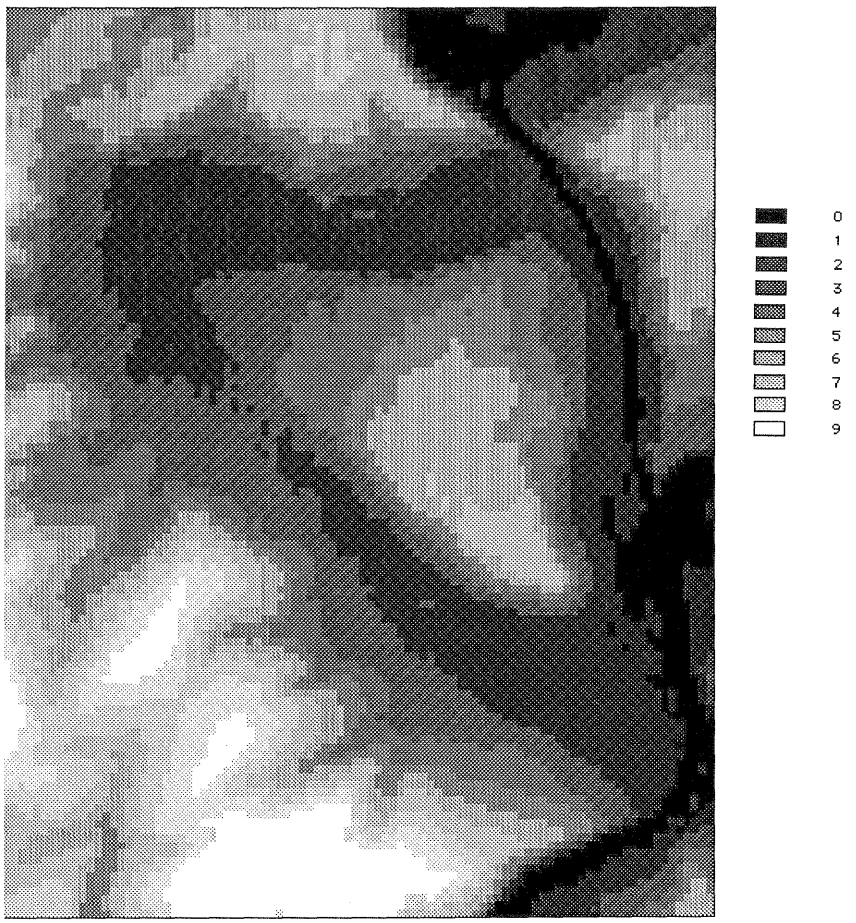

Figure 2: Digital elevation model with height classes (0 = 126-145 m, 1 = 146-165 m, 2 = 166-185 m, 3 = 186-205 m, 4 = 206-225 m, 5 = 226-245 m, 6 = 246-265 m, 7 = 266-285 m, 8 = 286-305 m, 9 = 306-325 m)

After this multiplication the long-term soil erosion for every pixel can bee seen (figure 3). This means that for each pixel that contain information in all of the layers (each represents one factor) a result is obtained. For pixels with missing information in one or more layers (for instance C-factor or K-factor) no result could be calculated.

For all pixels that contain the long-term soil erosion rates it is possible to assess exact values per pixel. Even small spatial changes and small areas can be evaluated.

Especially vineyards and crop-land show medium to high rates (as expected). All other land-use classes show rather small erosion rates.

Table 3 shows the correlation between slope and soil erosion rates in percent.

It is rather clear that with increasing slope also the soil erosion rate increases.

In table 4 one can see the correlation between depth of soil and soil erosion rates in percent.

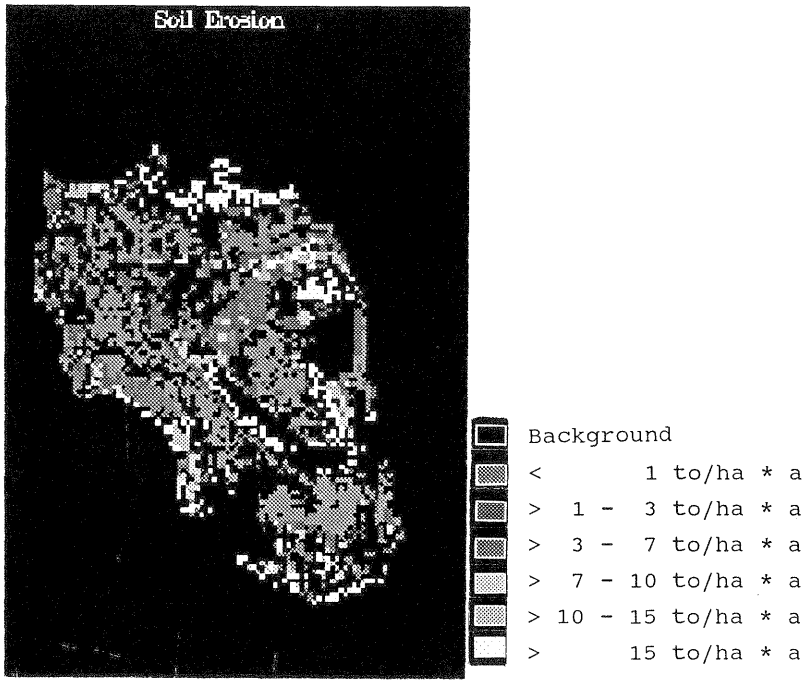

Figure 3: Long-term soil erosion rates

Table 2: Land use classes versus soil erosion classes

Land Use	No. of pix.	class 1 (in %)	class 2 (in %)	class 3 (in %)	class 4 (in %)	class 5 (in %)	class 6 (in %)
Meadow	1400	55,07	19,43	13,79	4,00	3,50	4,21
Dry Meadow	106	40,57	25,47	17,92	3,77	5,66	6,60
Wetland	173	72,83	8,09	9,83	4,05	4,62	0,58
Vineyards	318	2,20	8,18	4,40	2,52	2,83	79,87
Forest	560	42,32	17,68	16,25	6,25	8,39	9,11
Corn	13	23,08	0,00	0,00	30,77	23,08	23,08
Oats	84	21,43	14,29	16,67	7,14	5,95	34,52
Winter-Rye	18	44,44	0,00	0,00	5,56	5,56	44,44
Winter-Barley	28	25,00	14,29	10,71	10,71	3,57	35,71
Sommer-Barley	5	0,00	40,00	60,00	0,00	0,00	0,00
Water	-	-	-	-	-	-	-

class 1 = soil erosion > 1 to/ha*a
class 2 = soil erosion > 1 - 3 to/ha*a
class 3 = soil erosion > 3 - 7 to/ha*a
class 4 = soil erosion > 7 - 10 to/ha*a
class 5 = soil erosion > 10 - 15 to/ha*a
class 6 = soil erosion > 15 to/ha*a

Table 3: Mean slope versus soil erosion classes

Mean Slope (in %)	Erosion (in to/ha * a) < 1	> 1-3	> 3-7	> 7-10	> 10-15	> 15	Sum (in %)
2,5	93,63	4,86	1,24	0,09	0,18	0,00	100
8,5	20,00	44,60	21,49	3,35	1,86	8,70	100
20,0	0,00	7,34	28,50	15,21	13,99	34,97	100
49,0	0,00	0,00	2,08	4,69	16,67	76,56	100
86,5	0,00	0,00	0,00	0,00	0,00	100,00	100

Table 4: Soil depth versus soil erosion classes

Soil Depth (in cm)	Total (in %)	Erosion (in to/ha * a) < 1	> 1-3	> 3-7	> 7-10	> 10-15	> 15	Sum (in %)
< 30	60,84	60,84	10,84	12,59	1,40	4,55	9,79	100
31- 60	71,55	56,54	15,01	8,52	2,16	2,76	15,01	100
61-100	57,51	25,20	15,02	17,29	8,56	8,08	25,85	100
>100	87,28	46,98	22,96	13,37	4,97	3,43	8,28	100
	Tolerable soil erosion rates							

This reveals that especially the deep soils are not so affected by soil erosion as the shallow soils: About 61 % of the soils < 30 cm depth, about 72 % of the soils > 30 cm to 60 cm depth, about 58 % of the soils > 60 cm to 100 cm depth and about 87 % of the soils > 100 cm depth are not affected by soil erosion rates that are higher than tolerable according to SCHWERTMANN et al. 1987.

They give the following threshholds:
soils < 30 cm depth
1 t/ha * a
soils > 30 cm to 60 cm depth
3 t/ha * a
soils > 60 cm to 100 cm depth
7 t/ha * a
soils >100 cm depth
10 t/ha * a.

According to these threshholds a soil erosion risk map (figure 4) has been created that shows all the pixels that have higher soil erosion than tolerable in respect to soil depth.

This map shows mainly vineyards and steep slopes. For these areas effective soil erosion protection is necessary.

A simulation only for the affected vineyards shows that grass cover underneath the wine is a very effective protection against soil erosion.

Most of the pixels are no longer affected by high soil erosion rates! About 2/3 of the area show a soil erosion rate that is 2 or 3 classes lower than before! We cannot give the exact values in tons per hectar and year, since the classes are not equidistant. Anyhow, this is a significant reduction due to a simple protection measure.

6. CONCLUSION

This study shows that for a small area, the long-term soil erosion can be assessed with satellite data and ancillary digital data in a Geographic Information System.

For each pixel that is represented in all data layers it is possible to determine the soil erosion rates. Since all pixels are geocoded it is

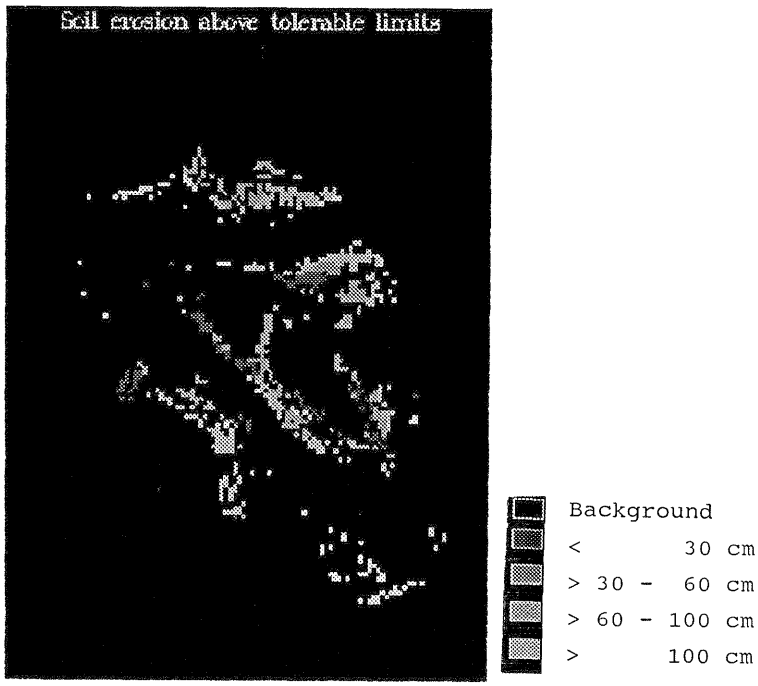

Figure 4: Soil erosion risk map

possible to guide soil erosion prevention measures precisely.

Especially vineyards and crop-land are areas with high soil erosion rates. This means that especially on intensively used areas with nutritious soils a lot of sediments and therefore a large amount of nutrients and herbicides are eroded that affect the water quality in the adjacent river.

In addition to the soil erosion assessment, the compiled GIS can also be used to simulate the effect of soil erosion protection measures (e.g. grass protection). It also allows to search for sites that are better suited for agriculture and vineyards in respect to soil erosion of course some other constraints have to be considered (e.g. climatic conditions).

We are now working on an automatic procedure to determine the slope length. After that stage we can use this method (when performed successfully for a small area) for larger areas to make more efficient use of the large coverage of satellite images.

7. ACKNOWLEDGEMENT

This study was funded by the Ministry of Public Worship and Instruction of Rheinland-Pfalz. We greatly appreciate this support.

8. REFERENCES

ARBEITSGRUPPE BODENKUNDE, 1982, Bodenkundliche Kartieranleitung.- 3. Aufl., Hannover.

BARSCH, D. & MÄUSBACHER, R., 1980, Auszugs- und Auswertungskarten als mögliche nutzungsorientierte Interpretation der Geomorphologischen Karte 1:25.000 (GMK 25). In: Berliner Geographische Abhandlungen, **31**, 31-48.

BERNSDORF, S., 1990, Eine geoökologische Bestandsaufnahme und Raumgliederung im Unteren Saartal. Anwendung und Bewertung des Konzeptes der Kartieranleitung Geoökologische Karte 1:25.000 (KA GÖK 25). Diplomarbeit, Universität Trier, unveröffentlicht.

FANDER, M., 1990, LANDSAT-TM- und SPOT-HRV-Daten als Grundlage für eine Landnutzungsklassifizierung. Eine vergleichende Untersuchung im Raum Frankfurt a.M. Diplomarbeit, Unviersität Trier, unveröffentlicht.

HENSEL, H. & BORK, H.R., 1988, EDV-gestützte Bilanzierung von Erosion und Akkumulation in kleinen Einzugsgebieten unter Verwendung der modifizierten Universal Soil Loss Equation. *Landschaftsökologisches Messen und Auswerten*, **2.2/3**, 107-136.

HEWER, Ch., 1989, Digitale Erfassung und Analyse bodenrelevanter Daten durch Geographische Informationssysteme. Diplomarbeit, Universität Trier, unveröffentlicht.

JÜRGENS, C., 1989, Nördliche Mandschurei. Satellitenbildinterpretation. In: Verlagsgruppe Bertelsmann GmbH (Ed.), 1989, Großer Internationaler Weltatlas, 269.

JÜRGENS, C., 1989, Vorschlag zur Abgrenzung von Trocken-, Normal- und Naßjahren anhand von Jahres- bzw. Halbjahresabflußsummen. *Deutsche Gewässerkundliche Mitteilungen* **33**, Heft 5/6, 189.

LANDESVERMESSUNGSAMT RHEINLAND-PFALZ, Ed., 1989, Das Digitale Höhenmodell des Landes Rheinland-Pfalz. Koblenz.

MEIJERINK, A.M., 1990, Summary report on ILWIS development. *ITC Journal* 1990-3, 205-214.

MEYNEN, E. & SCHMITHÜSEN, J., Hrsg., 1962, Handbuch der naturräumlichen Gliederung Deutschlands. (= Bundesanstalt für Landeskunde und Raumordnung), Bonn-Bad Godesberg.

MÜLLER, M.J., 1984, Erläuterungen zur Geomorphologischen Karte 1:25.000 der Bundesrepublik Deutschland. GMK 25 Blatt 15 6305 Saarburg. Berlin.

NEUFANG, L., AUERSWALD, K. & FLACKE, W., 1989, Automatisierte Erosionsprognose- und Gewässerverschmutzungskarten mit Hilfe der dABAG - ein Beitrag zur standortgerechten Bodennutzung. *Bayerisches landwirtschaftliches Jahrbuch*, Heft 7, 771-789.

RICHARDS, J.A., 1986, Remote Sensing Digital Image Analysis. (Berlin/New York, Springer).

RICHTER, G., 1965, Bodenerosion. In: Forschungen zur deutschen Landeskunde, **152**. Bonn-Bad Godesberg.

RICHTER, G., 1973, Schutz vor Bodenerosion - ein wichtiger Bestandteil des Umweltschutzes. *Geographische Rundschau*, **25**, 377-386.

RICHTER, G., 1976, Bodenerosion in Mitteleuropa. In: Wege der Forschung, **430**, 75-105. Darmstadt.

SCHMIDT, R.G., 1979, Probleme der Erfassung und Quantifizierung von Ausmaß und Prozessen der aktuellen Bodenerosion (Abspülung) auf Ackerflächen. In: Physiographica (= Baseler Beiträge zur Physiogeographie, **1**). Basel

SCHMIDT, R.G., 1988, Methodische Überlegungen zu einem Verfahren zur Abschätzung des Widerstandes gegen Wassererosion. (= Regio Basiliensis, **XXIX/1+2**, 111-121). Basel.

SCHULTZE, J.H., 1952, Bodenerosion in Thüringen. Ergänzungs-Heft **247** zu *Petermanns Geographischen Mitteilungen*.

SCHULZ, B.-S., 1988, Hypothesenfreie Landnutzungsklassifizierung aus LANDSAT 5-TM-Bilddaten. *Bildmessung und Luftbildwesen*, **56**, 89-97.

SCHWERTMANN, U., 1981, Die Vorausschätzung des Bodenabtrags durch Wasser in Bayern. Freising-Weihenstephan.

SCHWERTMANN, U., VOGL, W. & KAINZ, M., 1987, Bodenerosion durch Wasser. Vorhersage des Abtrags und Bewertung von Gegenmaßnahmen. Stuttgart.

WISCHMEIER, W.H. & SMITH, D.D., 1978, Predicting Rainfall Erosion Losses. A Guide To Conservation Planning. In: Agriculture Handbook **537** (= U.S. Department of Agriculture). Washington D.C..

WISS, H., 1988, Das Digitale Höhenmodell des Landes Rheinland-Pfalz. Zur Fertigstellung der ersten Ausbaustufe. Nachrichtenblatt der Vermessungs- und Katasterverwaltung Rheinland-Pfalz, Heft 2.